Folding model analysis for 240MeV ^{6}Li elastic scattering on ^{28}Si and ^{24}Mg

X. Chen, Y. -W. Lui, H. L. Clark, Y. Tokimoto, and D. H. Youngblood

In order to study giant resonance induced by ^{6}Li scattering, optical model (OM) analysis of ^{6}Li elastic scattering is necessary to get the optical parameters. OM has been widely used to analyze the heavy ion scattering data in term of empirical Woods-Saxon (W-S) parameterizations of the nuclear potential. However, it was found that a satisfactory microscopic understanding of heavy ion scattering can be obtained if one relates the optical potential to a fundamental nucleon-nucleon (NN) interaction through the double folding (DF) approach by folding this interaction with the nuclear matter distributions of both the target and projectile nuclei [1]. Since ^{6}Li is a loosely bound nucleus, breakup has a large contribution to the real part of the nuclear potential and is responsible for the substantial renormalization factor N_R for the real folded potential [2]. ^{6}Li elastic scattering itself is very interesting. ^{6}Li is in the mass number range A=4-12, where the elastic scattering show a transition between characteristics of light ions (A≤4) and characteristics of heavy ion (A≥12). Such data could provide a stronger test of the validity of any model for heavy ion potentials [3,4].

A beam of 240MeV ^{6}Li ions from the Texas A&M University K500 superconducting cyclotron bombarded self-supporting ^{28}Si and ^{24}Mg target foil in the target chamber of the multipole-dipole-multipole spectrometer. Elastic scattering and inelastic scattering to the low-lying states were measured from 5°-35°. The calibration procedures were described in details in Refs. [5,6]. The experimental cross sections were obtained from the charge collected, target thickness, dead time and known solid angle. The cumulative uncertainties in target thickness, solid angle, etc., result in about a ±10% uncertainty in absolute cross section.

Two different *NN* effective interactions (M3Y[7] and JLM[8]) were used to get the folded potential. Folding calculation **I** (FC**I**) used density dependent M3Y *NN* interaction and was described in detail by D.T. Khoa [9], while folding calculation **II** (FC**II**) with JLM effective interaction was described and discussed by F. Carstoiu *et al*. [10], L. Trache [11] and the references in these two papers. Two different density forms, Fermi distribution and Hartree Fork (HF) density [12], were used for target ground density during the folding procedures and are listed in Table I. The cluster-orbital shell-model approximation [13] form was used for ^{6}Li ground density with FC**I**. FC**I** was carried out with code DFPD4 [14] and elastic scattering data were fitted with code ECIS[15]. The optical parameters obtained are listed in Table II. FC**II** and the elastic scattering fit were carried out with code OPTJLM1[16]. HF densities were used for both target and projectile. The optical parameters are listed in Table III. The angular distributions of the calculated cross-section are plotted along with data in Fig.1 for ^{24}Mg and Fig.2 for ^{28}Si. Both FC**I** and FC**II** give almost the same quality fits for each nucleus. The FC**II** fit has large oscillations at large angles than the FC**I** fit.

A scaling factor on radius of the real optical potential is necessary to fit the elastic scattering for both ^{24}Mg and ^{28}Si when FC**I** is used. Different densities choices (as shown in Table I) will slightly change the value of the scaling factor (as shown in Table II.), but it can not

eliminate the factor. Different types of density dependent M3Y interactions such as CDM3Y4, CDM3Y5, CDM3Y6 [17] give almost the same scaling factors for ^{24}Mg elastic scattering. One possible reason for this factor could be the density used in the density dependent function. The density is defined as the sum of the densities of target and projectile, which may over-estimate the nuclear matter density at certain point.

DWBA calculations for ^{6}Li inelastic scattering to the low-lying 2^{+} state of ^{24}Mg and to low-lying 2^{+} and 3^{-} states of ^{28}Si were carried out with the optical parameter sets obtained by folding model **I**. CDM3Y5 density dependent NN interaction was used here and the Den1 form (as shown in Table I) was chosen as target density for both ^{24}Mg and ^{28}Si. The transition potentials were calculated with DFPD4 and the cross sections were calculated with ECIS. Deformation parameters for 2^{+} and 3^{-} states were obtained from electromagnetic B(EL) values by assuming the mass deformation length and coulomb deformation length are the same. The calculated angular distribution for the 2^{+} state in ^{24}Mg is plotted in Figure 3 along with the data. The calculated angular distributions for 2^{+} and 3^{-} states of ^{28}Si are plotted in Figure 4 and Figure 5 along with data. All the calculations of 2^{+} states agree well with the data. However, the DWBA calculation for the 3^{-} state of ^{28}Si does not agree well with the data as the calculated cross sections are slightly higher than the data.

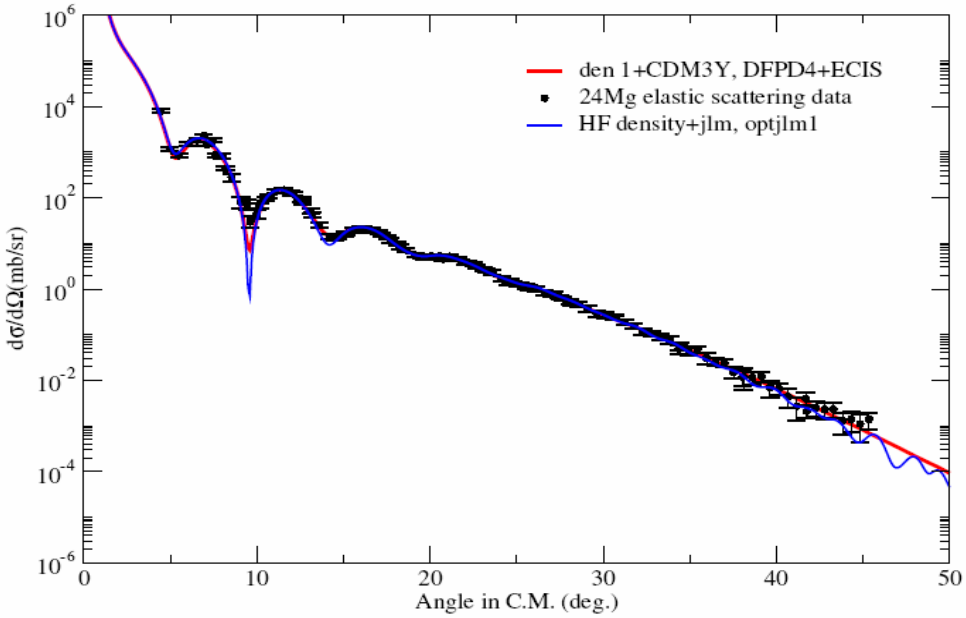

Figure 1. Angular distribution for ^{6}Li+^{24}Mg elastic scattering cross section. The red line shows the calculation using real folded potential with CDM3Y5 NN interaction and a W-S imaginary term. The blue line shows the calculation using both real and imaginary potential folded with JLM interaction.

TableI. Density parameters for different density choices. Den1 and Den2 are Fermi distributions. R_p, R_n, R_m, R_{ch} means the root mean square radii of the calculated proton, neutron, mass and charge distributions respectively.

target	Density choice	ρ_0	c	a	R_p	R_n	R_m	R_{ch}
^{24}Mg	Den1[18]	0.17	2.995	0.478	2.922	2.922	2.922	3.040
	Den2[19]	0.166	2.979	0.523	3.017	3.017	3.017	3.040
	HF	-------	-------	-------	2.928	2.906	2.917	3.000
^{28}Si	Den1[18]	0.175	3.15	0.475	3.010	3.010	3.010	3.875
	Den2[19]	0.167	3.155	0.523	3.123	3.123	3.123	3.154
	HF	-------	-------	-------	3.059	3.031	3.045	3.132

Table II. Optical model parameters obtained from fits of elastic scatterings with folding calculation **I**. N_r is renormalization factor for real potential. S_r is scaling factor for real potential radius. W,r_{i0},a_i are W-S parameters for imaginary potentials. J_v and J_w are the volume integral per nucleon pair for real and imaginary potentials respectively. σ_r is total reaction cross section.

Target	N-N int	Target density	N_r	S_r	W	r_{i0}	a_i	J_v	J_w	σ_r	χ^2
^{24}Mg	CDM3Y6	Den1	0.824	1.062	58.7	0.731	1.204	242	154	1799	1.038
	CDM3Y5	Den1	0.823	1.062	58.67	0.731	1.204	242	154	1799	1.039
	CDM3Y4	Den1	0.822	1.062	58.73	0.7311	1.204	242	154	1799	1.039
	CDM3Y5	HF	0.766	1.055	59.14	0.728	1.208	240	155	1803	1.042
	CDM3Y5	Den2	0.846	1.079	57.92	0.737	1.198	242	154	1793	1.032
^{28}Si	CDM3Y5	Den1	0.887	1.0624	41.33	0.9049	1.048	256	136	1757	1.461
	CDM3Y5	Den2	0.924	1.083	41.38	0.9049	1.046	258	136	1755	1.439
	CDM3Y5	HF	0.933	1.059	41.85	0.9011	1.051	257	137	1761	1.485

Table III. Optical potential parameters obtained from the fit of elastic scatterings with folding calculation **II** .N_r and N_w are the normalization factor for real and imaginary potential respectively. t_r and t_w are range parameters for real and imaginary potential respectively.

Target	N-N int.	target density	N_r	t_r	N_w	t_w	J_v	J_w	σ_r	χ^2
^{24}Mg	JLM	HF	0.519	0.9559	0.862	2.586	237	144	1803	1.6
^{28}Si	JLM	HF	0.546	0.9165	0.825	2.4275	248	137	1734	1.94

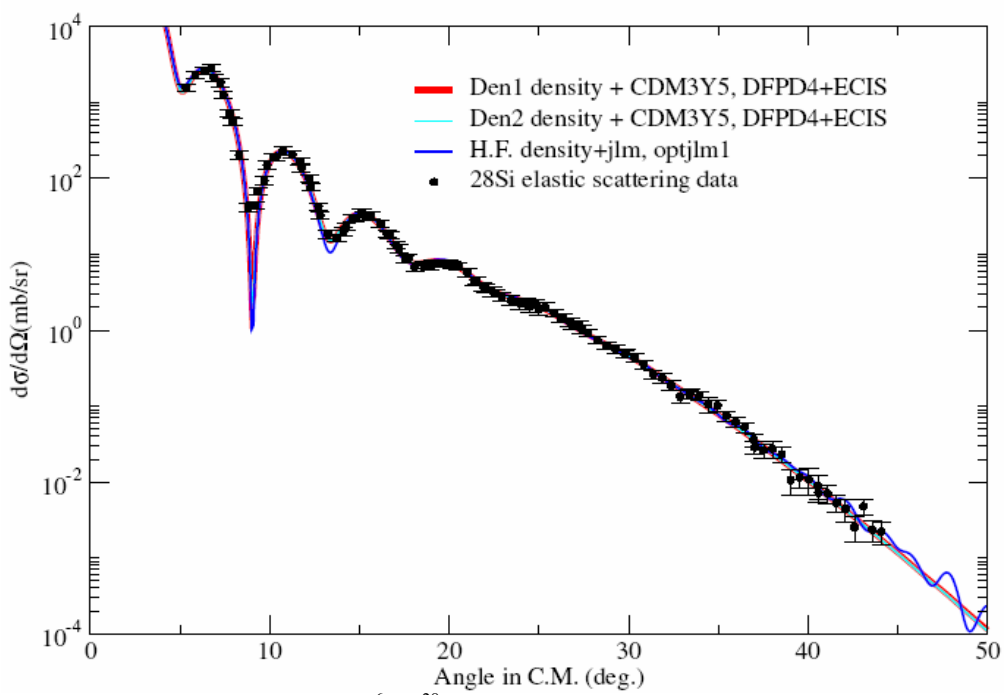

Figure 2. Angular distribution for ^{6}Li+^{28}Si elastic scattering cross section. Both red and cyan lines show the calculation using real folded potential with CDM3Y5 N-N interaction and a W-S imaginary term. Den1 density is used for red line and Den2 density is used for cyan line. The blue line shows the calculation using both real and imaginary potential folded with JLM interaction.

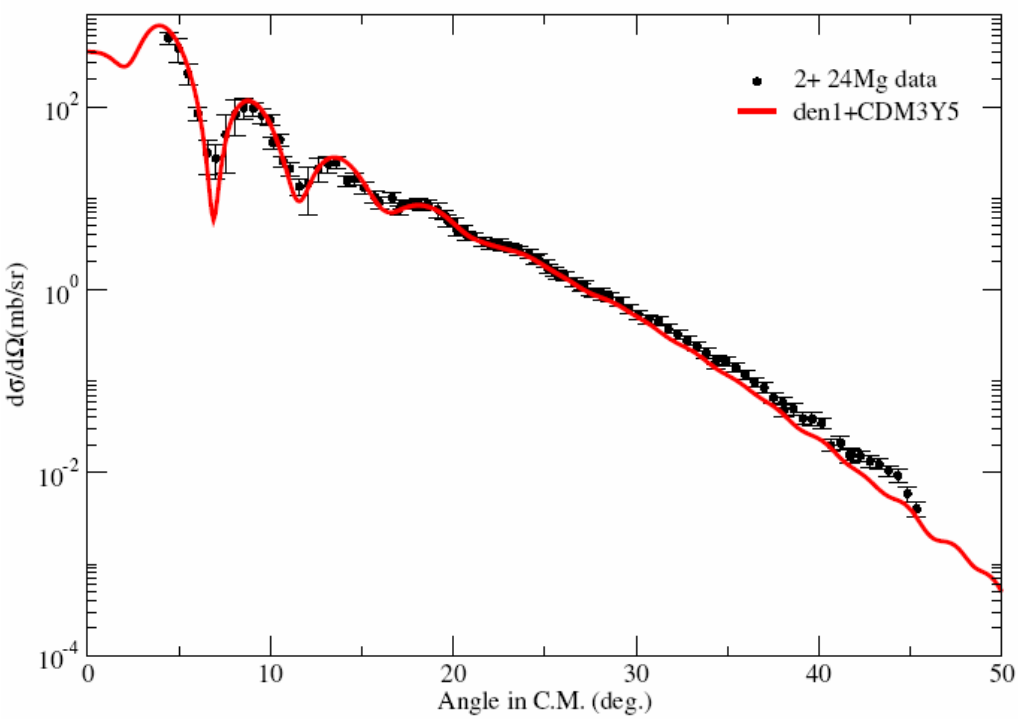

Figure 3. The line shows the calculated differential cross section using CDM3Y5 NN interaction for inelastic scattering to the 1.369MeV 2^{+} state in ^{24}Mg plotted versus average center-of-mass angle along

with the data points. The electromagnetic B(E2) value [20] was used and the corresponding deformation length δ=1.978fm.

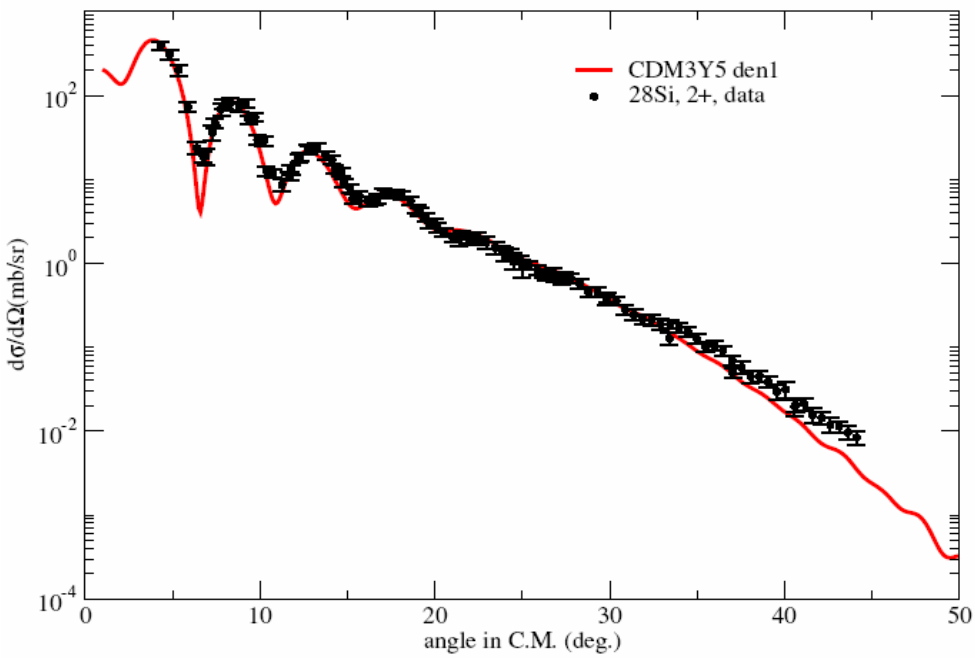

Figure 4. The line shows the calculated differential cross section using CDM3Y5 NN interaction for inelastic scattering to the 1.779MeV 2^+ state in ^{28}Si plotted versus average center-of-mass angle along with the data points. The electromagnetic B(E2) value [20] was used here and the corresponding deformation length δ=1.426fm.

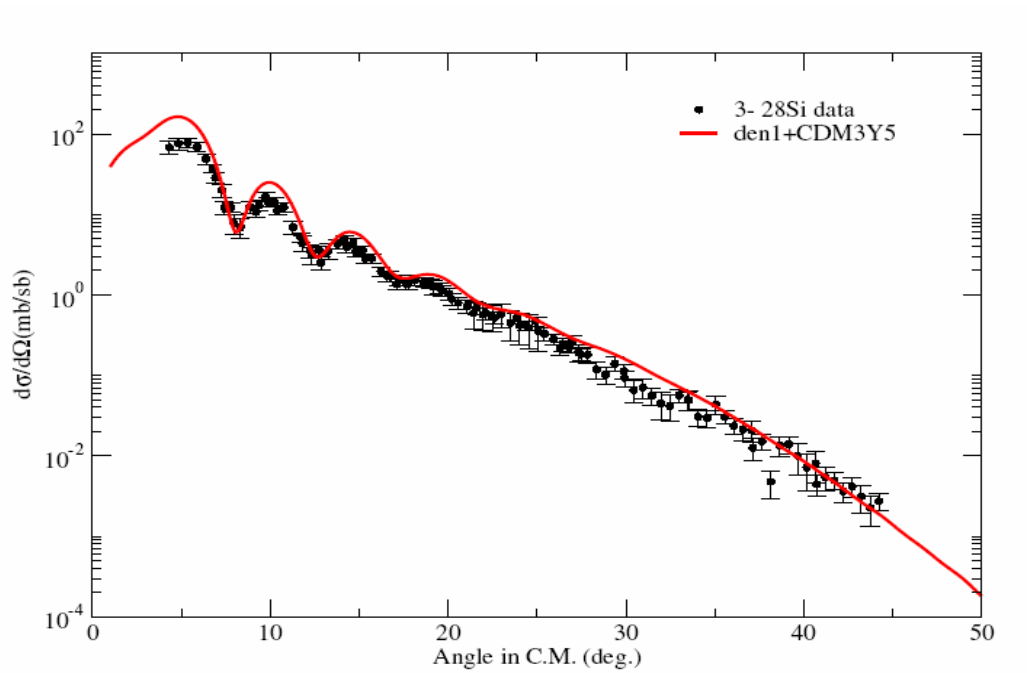

Figure 5. The line shows the calculated differential cross section using CDM3Y5 NN interaction for inelastic scattering to the 6.879MeV 3^- state in ^{28}Si plotted versus average center-of-mass angle along with the data points. The electromagnetic B(E3) value [21] was used here and the corresponding deformation length δ=1.336fm.

We thank Dr. Livius Trache and Dr. Florin Carstoiu for their help in JLM folding calculation. We thank Dr. D.T.Khoa and Mr. Hoang Sy Than for their help and offer of the computer codes to do the CDM3Yn folding calculation and cross-section calculation.

[1] G. R. Satchler and W. G. Love, Phys. Rep. **55**, 183(1979).

[2] Y. Sakuragi, Phys. Rev. C **35** 2161 (1987); Y. Sakuragi, M. Yahiro, M. Kmimura, Prog. Theor. Phys. Suppl. **89** (1986) 136; Y. Sakuragi, M. I. Hirabayashi, M. Kamimura, Prog. Theor. Phys. **98** 521(1997).

[3] R.M. DeVries, *et al.*, Phys. Rev. Lett. **39** 450 (1977).

[4] M. El-Azab Farid, M.A. Hassanain, Nucl. Phys. **A678**, 39 (2000).

[5] D. H. Youngblood, Y. -W.Lui, H. L. Clark, P. Oliver, and G. Simler, Nucl. Instrum. Methods Phys. Res. **A361**, 539 (1995).

[6] H. L. Clark, Y. -W.Lui, and D. H. Youngblood, Nucl. Phys. **A589**, 416 (1995).

[7] G. Bertsch, J. Borysowicz, H. McManus and W. G. Love, Nucl. Phys. **A284**, 399 (1977).

[8] J. P. Jeukenne, A. Lejeune, and C. Mahaux, Phys. Rev. C **16**, 80(1977).

[9] Dao T. Khoa and G. R. Satchler, Nucl. Phys. **A668**, 3 (2000).

[10] F. Carstoiu, L. Trache, R. E.Tribble and C. A. Gagliardi, Phys. Rev. C **70**, 054610 (2004).

[11] L. Trache, *et al.*, Phys. Rev. C **61**, 024612 (2000).

[12] M. Beiner and R. J. Lombard, Ann. Phys. **86**, 262 (1974); F. Carstoiu and R. J. Lombard, ibid. **217**, 279 (1992).

[13] A. Korshenninnikov, *et al*., Nucl. Phys. **A617**, 45 (1997).

[14] D.T. Khoa, unpublished.

[15] Jacques Raynal, Computing as a Language of Physics, ICTP International Seminar Course, Trieste, Italy, Aug. 2-10, 1971 (IAEA,1972), p281; M.A. Melkanoff, T. Sawada and J. Raynal, Methods in Computational Physics.**6**: Nuclear Physics (Academy Press, New York, 1966) p1.

[16] F. Carstoiu, unpublished.

[17] D. T. Khoa, G. R. Satchler and W. von Oertzen, Phys. Rev. C **56**,954 (1997).

[18] M. Pignanelli *et al.*, Phys. Rev. C**33** 40(1986).

[19] G. Fricke *et al.*, Atomic Data and Nuclear Data Tables **60**, 177 (1995).

[20] S. RAMAN, C. W. NESTOR, JR., and P. TIKKANEN, At. Data Nucl. Data Tables **78**, 1 (2001).

[21] T. KIBEDI and R. H. SPEAR, At. Data Nucl. Data Tables **80**, 35 (2002).